JOURNAL OF MATERIALS SCIENCE 19 (1984) 1171–1177

The detailed structure of delamination fracture surfaces in graphite/epoxy laminates

T. JOHANNESSON, P. SJÖBLOM, R. SELDÉN*
Linköping Institute of Technology, Division of Engineering Materials, Department of Mechanical Engineering, S-581 83 Linköping, Sweden

Delamination fracture surfaces of angle-ply graphite/epoxy specimens failed in tension were studied in the SEM. The fracture surfaces contain resin-rich and resin-poor areas, with the former showing imprints from fibres while the latter show debonded fibres. A delamination crack propagates in the outer parts of the plies adjacent to the resin-rich interlaminar region and alternates from one ply to the adjacent ply and back as it propagates. The serrations formed in between fibres in the outermost parts of plies are tilted. The sense of the tilt is in agreement with the direction of the major tensile principal stress. The delamination is suggested to proceed in steps including debonding of fibres, crack opening by the major principal tensile stress and linking together of these fractures.

1. Introduction

The mechanism of delamination has been the subject of several studies. Rotem and Hashin [1] in their study of the failure process of angle-ply laminates identified delamination as the major failure mechanism for ply angles $\theta < 45°$.

Reifsnider *et al.* [2] presented an experimental study of delamination in two quasi-isotropic graphite/epoxy (AS/3501) laminates of different lay-up sequences. The delamination process was recorded by photography and video-monitoring. Delamination occurred due to normal tensile stresses, σ_z, and occurred together with transverse cracking. The onset of delamination, however, could not be predicted. Several investigators have tried to apply fracture mechanics to the failure of laminated fibre composites. The results show only limited success. According to Peters [3] successful applications could only be expected for failure occurring purely by delamination where the condition of self-similar crack growth seems to be fulfilled. Morris [4] studied delamination fracture surfaces and related some of the features observed on these surfaces to the fracture process.

In the present work, delaminated fracture surfaces of graphite/epoxy angle-ply specimens are investigated and the microscopic structural features are analysed in order to understand the mechanisms of delamination. Scanning electron microscopy (SEM) is used for the fracture surface analysis.

2. Experimental procedure

Unidirectional carbon/epoxy prepreg, T300/1034, with a matrix content of approximately 42% by volume was used as starting material. The Fiberite system, Hy-E 1034, is essentially a tetraglycidyl 4,4′ diaminodiphenyl methane epoxide (TGMDA or TGDDM) with curing agent 4,4′ diaminodiphenyl sulphone (DDS) and a catalyst borontrifluorine monoethylamine (BF_3-MEA). It contains as a second epoxide diglycidylether of bisphenol A (DGEBA).

The prepreg materials were hand laid-up and fabricated following the manufacturer's recommended curing procedure. The final product was obtained as rectangular sheets with a final matrix volume content of approximately 35%. Specimens

* Present address: Swedish Plastics and Rubber Institute, Bultgatan 5, S-852 47 Sundsvall, Sweden.

0022–2461/84 $03.00 + .12

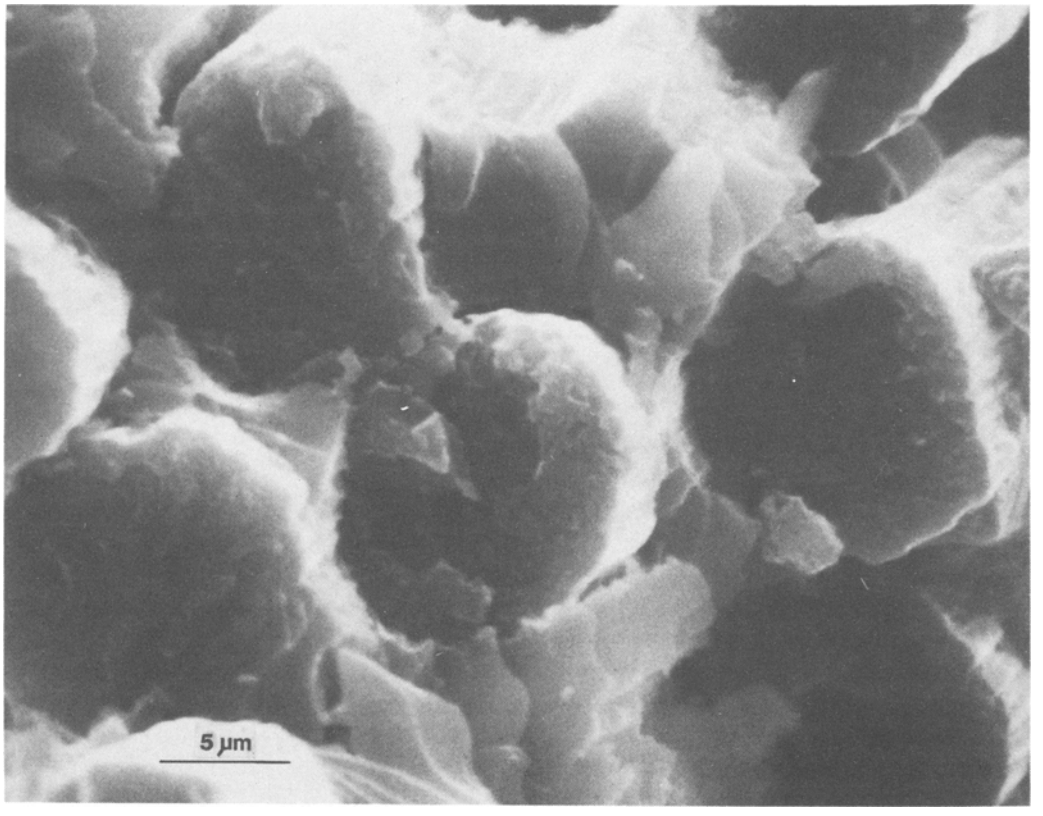

Figure 1 Fibre failures in an angle-ply ($\theta = \pm 15°$). Fibres have failed under tension and resin by cleavage (SEM).

for tensile testing were cut out using a diamond wheel. The thickness of the specimens was approximately 1 mm corresponding to eight prepreg layers laid up according to $[\pm\theta]_{2s}$, with $\pm\theta = 5$, 15, 30, and 45°.

The specimens were tested in tension using a MTS universal testing machine. The stress–strain properties were recorded and stored in a computer. In order to understand the process leading to ultimate failure, failure event sequences were recorded using motordriven cameras, taking six frames per second. The result of the failure event analyses has been presented elsewhere (5).

Prior to SEM examination, the fractured specimens were cut with a diamond wheel to smaller pieces, and carbon was evaporated in vacuum onto the fracture surfaces to minimize static charging by the SEM electron beam.

The microscope used for fracture analysis was a Jeol JSM P 15 scanning electron microscope.

3. Results and discussion

The stress–strain curves of the laminates tested except the $[\pm 45]_{2s}$ specimens are characteristic of a brittle material. The $[\pm 45°]_{2s}$ specimens show a more ductile behaviour [5].

Fracture surfaces with fibre failures show a relatively small amount of fibre pull-out and some resin residues on the pulled-out fibre surfaces indicating a relatively high interfacial bond strength. The fibre failures are characteristic of tensile failure and the resin fracture surfaces in between the fibres are smooth, indicative of cleavage failure (Fig. 1). The delamination fracture surfaces show a number of interesting features (Figs. 2 to 5). A general delamination fracture surface has three main constituents; uncovered fibres, imprints from fibres that have delaminated and the characteristic structure of the fractured epoxy matrix. This matrix structure was first reported by Chamis and Sinclair [6] who named them lacerations. They are also known as hackles or serrations [4, 7]. The term "serrations" will be used throughout this text. Important to notice in Figs. 2 to 5 is that the serrations always tend to align more or less perpendicular to the fibre imprints (or uncovered fibres).

Figure 2 Delamination fracture surface in an angle-ply laminate ($\theta = \pm 15°$). The surface is "resin rich" consisting of imprints from debonded fibres and resin failures (serrations) (SEM).

Some areas observed on a delamination fracture may be characterized as "resin rich" as few fibres are seen (Fig. 2). These areas consist mainly of imprincts of fibres and serrations in between them. Other areas show relatively little resin residue ("resin poor"). In this case, the main constituents are uncovered fibres with some matrix structure in between. In some fracture surfaces, resin-rich areas are dominant and in others, resin-poor areas are dominant.

Usually, however, one finds both uncovered fibres and fibre imprints on the same surface, as shown in Fig. 3 for two mating surfaces. Imprints on one surface corresponds to uncovered fibres on the other (and vice versa).

These observations are interpreted as an indication that there are two preferred paths for the delamination crack, one along each side of the interlaminar region. A two-planar fracture surface thus results where the location of the crack propagation alternates from one side of the interlaminar region to the other.

A closer inspection of the areas with serrations give further information. Figs. 4a and b show a delamination fracture surface at 90° and 30° to the electron beam of the SEM, respectively. The serrations are plate-like features standing almost perpendicular to the fracture surface. It is seen that the formation of serrations has taken place in between the outermost fibres of the ply rather than in the resin-rich interlaminar region itself.

Inspection of Figs. 2 to 5 reveals that the serrations have a general tilt with respect to the plane of the laminate as indicated in Fig. 6. It can also be seen that the tip of the serrations are bent slightly. The direction in which the tips are bent coincide with the direction of relative motion of the adjacent plies at delamination.

Finally, it should be noted that the serrations are subdivided into finrer structures near the fibres or the fibre imprints (Figs. 2 to 5). These structures look like river patterns observed on fracture surfaces of brittle materials [8]. These "serration feet" usually appear on one side of the serrations

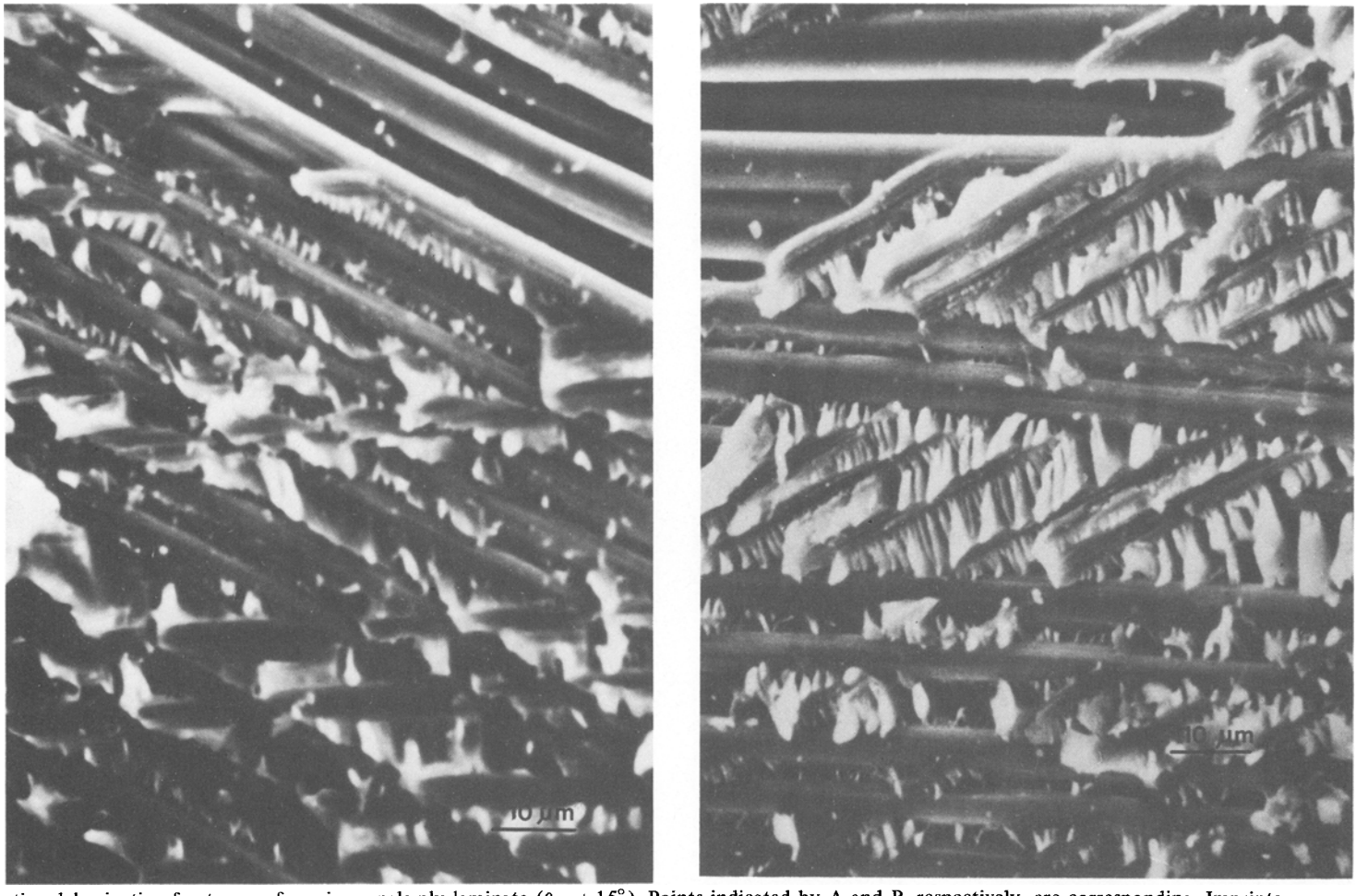

Figure 3 Two mating delamination fracture surfaces in a angle-ply laminate ($\theta = \pm 15°$). Points indicated by A and B, respectively, are corresponding. Imprints on one corresponds to bare fibres on the other and vice versa (SEM).

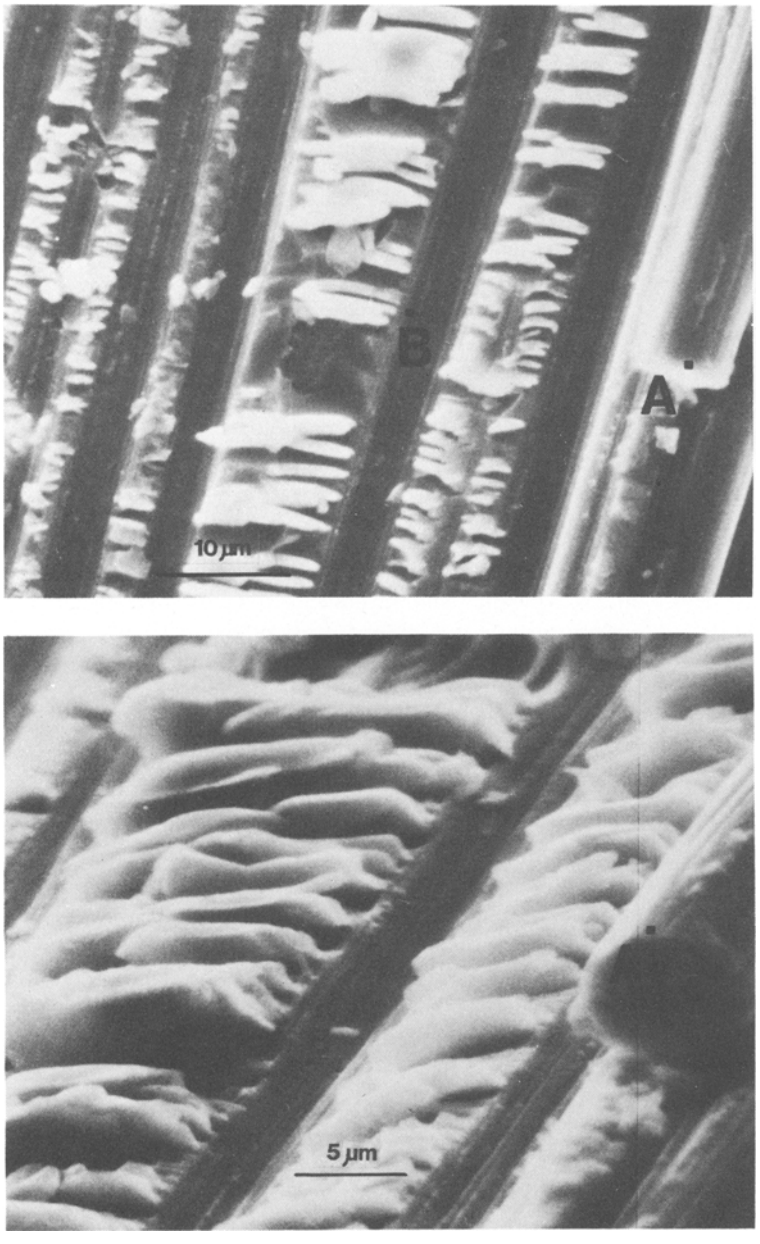

Figure 4 Delamination fracture surface in an angle-ply laminate ($\theta = \pm 5°$). (a) Surface perpendicular to the electron beam, (b) Surface tilted to 30° to the electron beam (SEM).

(Fig. 3b) whilst the other side has a coarser structure. Sometimes, however, the feet occur on both sides of the serrations. In Fig. 5, the serrations show an intricate structure. There is a region to the left in which the serrations in between debonded fibres seem to overlap. A plausible explanation of this is that the fibre–matrix interfaces debonded first. The microscopic crack then propagated from the broken fibre–matrix interfaces into the resin. The cracks have, however, failed to match up and an overlap region is created. The crack front, viewed on a microscopic scale, thus propagates from the fibre–matrix interfaces into the resin. The relation between the morphology of the "serration feet" and the microscopic crack propagation direction is thus the same as for river patterns observed in metals.

A mechanism for the formation of serrations has been suggested by Morris [4]. For a more detailed understanding, the effect of the stress state at the site of the delamination has to be taken into account. According to Pipes and Pagano [9], the essential stress components acting in the interlaminar region near the edge of an angle-ply

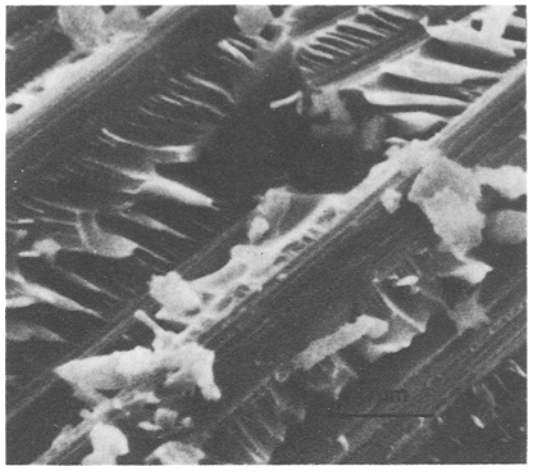

Figure 5 Delamination fracture surface in an angle-ply laminate ($\theta = \pm 5°$).

specimen is τ_{xz} and σ_x. This will yield a major principal stress in the x, z-plane along a direction of 45° or less from the x, y-plane (Fig. 7). The observed tilt of the serrations agrees well with the assumption that the major principal stress opens up microcracks in the brittle matrix perpendicular to the direction of that stress. This conclusion, is however, only qualitative.

In summary, the process of delamination is suggested to occur in the following steps:

(a) fibres debond, probably due to stress concentrations at the interfaces

(b) slant cracks are formed in the resin perpendicular to the major principal stress

(c) debonded regions and slant cracks are linked together by microscopic crack propagation from the broken interfaces into the resin.

4. Conclusion

Delamination fracture surfaces consist partly of debonded fibres and partly of resin failure in the form of serrations. The serrations are formed in the outer parts of the plies adjacent to the interlaminar resin-rich region, rather than within this region. The delamiantion crack thus propagates alternating close to one or the other ply, giving a two-planar fracture surface.

Delamination is a process occurring in several steps including debonding the fibres in the resion, crack linking by crack growth from the fibre/matrix interfaces into the resin.

The detailed structure of the serrations depend on the stress state at failure and the failure mode. The serrations are formed from microcracks with their planes perpendicular to the tensile major principal stress. The tips of the serrations are deformed along the direction of relative motion of the surfaces at delamination.

It is oversimplication to consider delamination to occur by self-similar crack propagation in the resin-rich region.

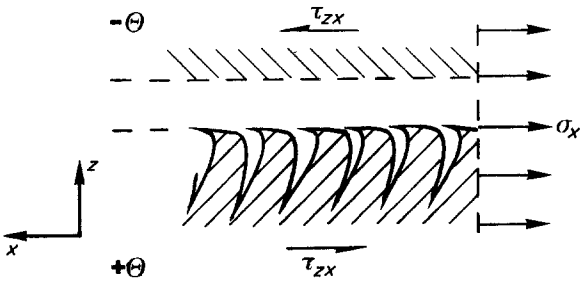

Figure 6 Sketch of the edge view of the serrations in relation to the dominating stresses.

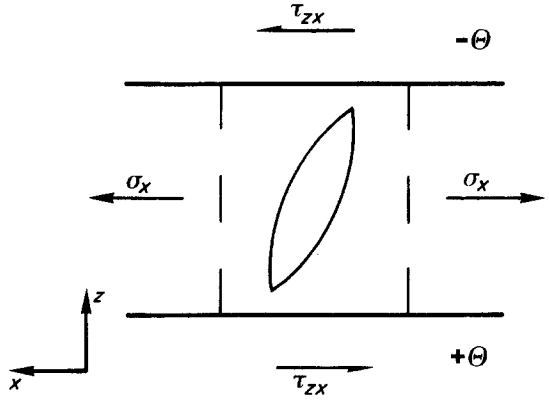

Figure 7 Sketch of the brittle microcracks that are suggested to open up by the dominating stresses.

Acknowledgement

This study is supported financially by the Swedish National Board for Technical Development (STU) under contract Nr 81-5214 and is performed within the Fiber Composites Research Group at Linköping Institute of Technology. Discussions with Professor T. Hahn have been most valuable.

References

1. A. ROTEM and Z. HASHIN, *J. Compos. Mater.* 9 (1975) 191.
2. K. L. REIFSNIDER, E. G. HENNEKE and W. W. STINCHCOMB, ASTM-STP 617 (American Society for Testing and Materials, Philadelphia, 1977) p. 93.
3. P. PETERS, *J. Compos. Mater.* **12** (1978) 250.
4. G. E. MORRIS, ASTM-STP 696 (American Society for Testing and Materials, Philadelphia, 1978) p. 274.

5. P. SJÖBLOM, R. SELDÉN and T. JOHANNESSON, Linköping Institute of Technology, Report LiTH-IKP-R-234 (1982).
6. J. H. SINCLAIR and C. C. CHAMIS, NASA Technical Paper 1081, National Aeronautics and Space Administration, Washington DC (December 1977).
7. J. AWERBUCH and H. T. HAHN, ASTM-STP 723 (American Society for Testing and Materials, Philadelphia, 1981) p. 243.
8. "Metal Handbook" Vol. 9, edited by J. A. Fellows (American Society for Metals) (1974) p. 64.
9. R. B. PIPES and N. J. PAGANO, *J. Compo. Mater.* 4 (1970) 538.

Received 21 March
and accepted 21 July 1983.